J. Condensed Matter Nucl. Sci. 22 (2017) 35–46

Research Article

Oscillating Excess Power Gain and Magnetic Domains in NANOR®-type CF/LANR Components

Mitchell R. Swartz*

Nanortech Inc., Wellesley Hills, MA 02148, USA

Abstract

Post-magnetization effects, both significant and time-variant, were observed in NANOR®-type CF/LANR components. In contrast to previously observed exponential falloffs of sample activity (peak incremental excess power gain), post-magnetization activity demonstrates oscillatory activity. This paper reports an analysis of the force density and expected theoretical frequency for oscillations, which have already been observed to exist between these magnetic domains after magnetization, calculated by using the Maxwell stress tensor.

Keywords: LANR, Magnetic domains, Magnetism, NANOR®, Oscillating power gain

---

1. Introduction – NANOR®-type CF/LANR Dry Preloaded Components

A NANOR®-type component is a hermetically sealed CF/LANR (cold fusion/lattice assisted nuclear reaction) nanomaterial, preloaded and arranged as a two-terminal electrical component which can yield significant heat (Figs. 1 and 2). They are designed to avoid leakage, enable stabilization and activation of the contained nanostructured alloyed material. As a result, the NANOR®-type preloaded component [1,2] has been like the proverbial "lab rat" for several papers, and was also the central component in an open demonstration at MIT in 2012 ([3]; which is one of the locations where the "normal" (unexposed to magnetization effects) exponential fall off of CF/LANR activity was followed over months). The papers include investigations of material science [4–6] and radiation physics [5,6,8], which have revealed several electrical transconduction states. Most importantly, of these transconduction states, only one produces the desired trait known as "excess heat" [7]. We begin by considering how the activity of these components is measured, and then how they are affected by the applied magnetic field intensity, and finally what may cause the post-magnetic activity-oscillations.

---

*Dr. Mitchell R. Swartz ScD, MD, EE, E-mail: nanors@nanortech.com.

2. Methods

2.1. Determination of activity of NANOR®-type components

The preloaded NANOR®-type components are driven by a high voltage circuit (up to 3000 V peak). In addition to using several types of commercial calibrations, we augment the calibrations using Keithley picoammeters (Types 480 and 486) and Keithley current sources (Type 225). For voltage measurements, Keithley electrometers (610B,610CR,602) and HP5334, HP3490, and Keithley multimeters were used. Voltage sources include HP-Harrisons, Kepco, and VWR. The input voltage was delivered in every run alternatively to the NANOR® and the ohmic control which was at the same location and used to thermally calibrate the system [9–11].

Input power is defined as $V \times I$. There is no thermoneutral correction in the denominator. Therefore, because consideration of loss by possible recombination is not removed, the observed power is a lower limit [12]. The energy calculations are also calibrated by time integration for additional validation. The instantaneous power gain (non-dimensional power amplification factor [10.11,13]) is defined as $P_{\text{out}}/P_{\text{in}}$. When present, the excess energy is defined as $(P_{\text{output}} - P_{\text{input}}) \times$ time. Data acquisition is taken from voltage and current sensors, and temperatures and heat flux sensors at multiple sites of the system. Data sampling is at 0.20 – 1 Hz, with 16–24^{+} bit resolution, a voltage accuracy of $0.015^{+/-0.005}$ V, and a temperature accuracy of <0.6 degrees C. The noise power of the Keithley current sources driving the reactions is generally ~10 nW.

After driving the component and the control in each run, their power and energy gain were separately determined both by power-normalized delta-T (dT/ P_{in}), and input power normalized increase in heat flow (delta-HF/P_{in}), and the directly by semiquantitative calorimetry [2,3]. In semiquantitative calorimetry, the amount of output energy is directly determined from the heat release, which is then compared to the input energy. The excess heat-producing activity can be determined by comparing the output of the NANOR® type component to the output of the precisely driven ohmic control, as demonstrated in the middle of Fig. 1.

2.2. Magnetization of NANOR®-type components

For what is reported here, the applied magnetization sequence consisted of rapidly repeating pulses of an intense >2 Tesla magnetic field intensity [4]. The applied magnetic field intensity, thus, highly fractionated with 3500 pulses delivered, each with a rise time of <0.1 ms, followed by an intra-pulse delay of one second.

3. Results

3.1. Response without applied magnetic field

Figure 1 shows the responses of these CF/LANR NANOR®-type components with any applied magnetic field intensity in three graphs of the same experimental run. A determination of the presence of excess heat can be made by comparing the output for NANOR®-type LANR component to the thermal (ohmic) control. The top of Fig. 1 shows the electrical input power and the incremental output temperature rise (defined as "delta-T"). The x-axis represents time. The y-axis on the left-hand side represents electrical input power in watts. The y-axis on the right-hand side represents delta-T. The calibration pulses, used for accuracy and precisions checks of voltages and currents and time, are also shown. The middle of Fig. 1 includes the same data but the incremental output temperature rise is normalized to the input power by dividing by the input power. This metric has delta-T/P_{in} be a nearly straight horizontal line for the ohmic control; which facilitates semiquantitative measurements by use of a simple ratio. The bottom of Fig. 1 is a full calorimetric presentation showing the input power and energy and output power and heat (energy) from the ohmic control and the NANOR®-type component at several input powers. The y-axis on the left-hand side represents electrical input power in watts. The y-axis on the right-hand side is the time-integrated amount of energy delivered at

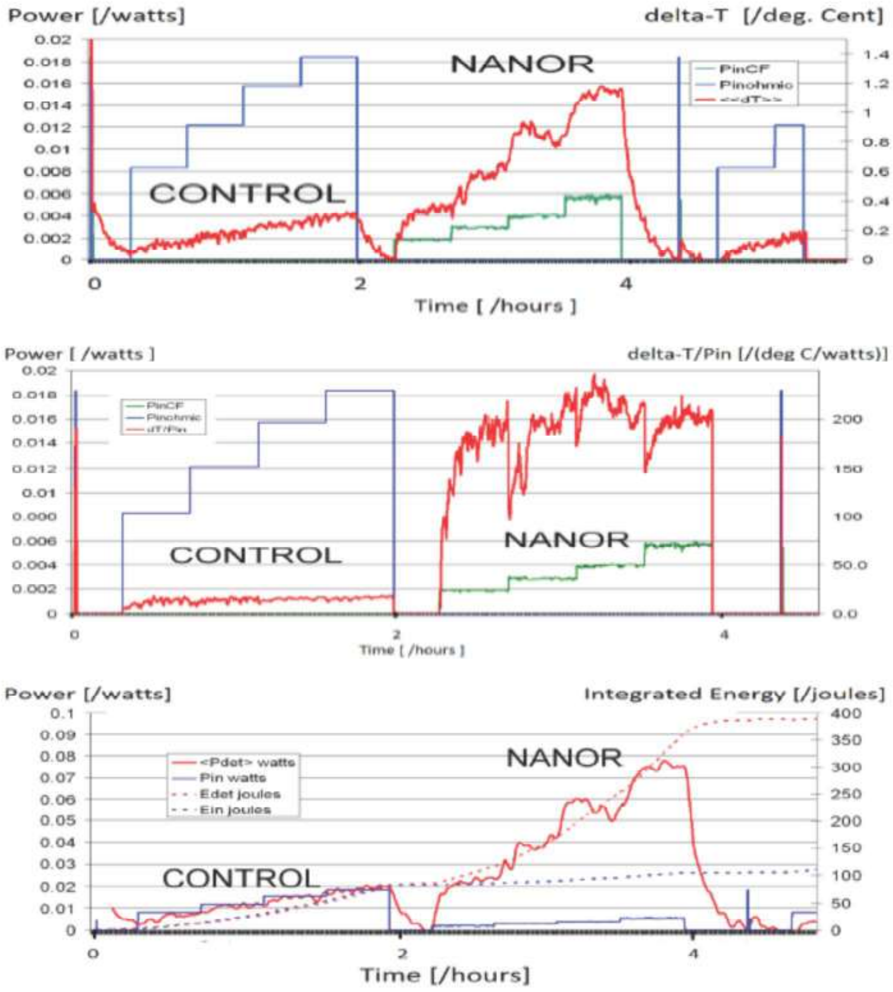

Figure 1. Response of a control and NANOR®-type component – No magnetic field. This figure shows three different ways of evaluating the possible presence of excess energy from a single run of an ohmic control and a NANOR®-type component. The ohmic control was driven first and then the component was electrically driven, as marked (*top*). The electrical input power and resultant delta-T for the ohmic control and then the NANOR®-type component are shown (*middle*). The electrical input power and resultant delta-T normalized to the input power (delta-T/P_{in}). Importantly, this linearizes the output and enables calculation of power gain. In contrast to the graph on the top, this metric is a nearly straight horizontal line for the ohmic control (*bottom*). Calorimetric presentation of the input power and energy and output power and heat for the ohmic control and the NANOR®-type component.

input, and then released. The lighter energy curves (dots) are read off of the right-hand side y-axis, which represents the amount of energy released in joules.

Thus, these calorimetric curves rule out energy storage, chemical sources of the induced heat, possible phase changes, and other sources which might interfere with obtaining semiquantitative results.

Figure 2 shows the calorimetric responses of both the ohmic control and the preloaded NANOR®-type compo-

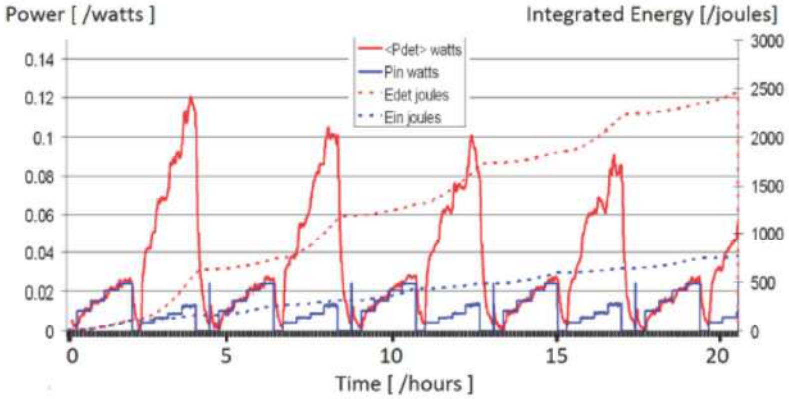

Figure 2. Reproducibility of a NANOR®-type component – No Magnetic Field. This is a calorimetric presentation of an experimental run, discontinuous with Fig. 3, with more than four cycles. The electrical input power and energy and output thermal power and heat are shown alternatively both from the ohmic control and the NANOR®-type component at several input powers. This component and control had NOT been driven in the presence of an applied magnetic field intensity, unlike Figs. 3 and 4.

nent over four complete cycles, at four different input electrical power levels. Figures 1 and 2 show that the active preloaded CF/LANR component has significant improvement in thermal output compared to a standard ohmic control (a carbon composition resistor). They also demonstrate that excess heat was produced only during energy transfer to the NANOR®-type LANR component heralding clearly over-unity thermal output power from it. Figure 2 demonstrates the reproducibility of the ohmic control and the near reproducibility of the NANOR®-type component over several cycles. In Fig. 2 the peak power gain of the NANOR®-type component slowly decreases, in a regular way, over time.

Figure 2 also demonstrates an exponential falloff of the peak incremental excess power gain. It is important to note that this component had NOT been driven in the presence of an applied magnetic field intensity, versus what is shown in Fig. 3. Contrast this exponential, slowly decreasing response, which is what was always seen [1–5], to the newly observed irregular, somewhat oscillatory-like, activity which occurred only after the components were exposed to the H-field, and only while an applied E-field was used to activate the CF/LANR component (Figs. 3 and 4).

3.2. Unique response after magnetic field

3.2.1. *Introduction – Magnetic responses in CF/LANR systems*

Previously, magnetic [14–16] and radiofrequency electromagnetic [17] effects have been reported in aqueous CF/LANR systems. In aqueous CF/LANR systems, steady magnetic fields have a small inhibitory effect on loading electrolysis when the applied H-field is perpendicular to the direction of the electrical currents [16]. In dry, preloaded CF/LANR systems, at higher electrical drive currents to the component, time-varying alternating magnetic fields simultaneously applied, induce small to significant increase gains in the activity [4] and some changes are long-lasting. Therefore, magnetically treated NANOR®-type components are called M-NANOR®-type components by our group to distinguish them and anticipate their unique oscillating-activity behavior and other longer term effects (Figs. 3 and 4).

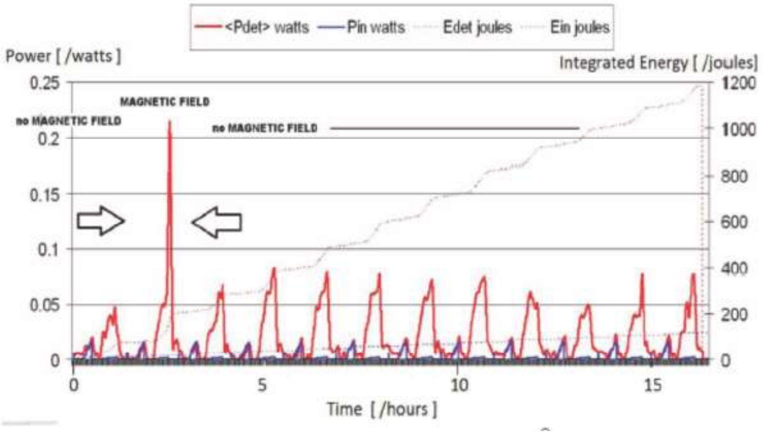

Figure 3. Impact of an H-field on the behavior of a NANOR®-type component. This experimental runs shows the impact of an applied H-field on the activity of a NANOR®-type component before, during and after, a single sequence of fractionated high intensity magnetic field application between the arrows. At all other points in time there were NO additional large applied magnetic field intensity. Note the absence of an exponential or linear fall-off of peak activity.

3.2.2. *Synchronous magnetically induced increased energy gain*

During the first magnetic-NANOR® run, we were quite surprised by the different responses of the NANOR® component during *and after* $\mathrm{d}H/\mathrm{d}t$ coercing. It was discovered that for magnetic interactions with active nanostructured CF/LANR systems [4], there is enhanced improvement of LANR (which occurs at the same time as the magnetization and therefore is called "synchronous"). As a result of the magnetization sequence, there appeared a significant increase

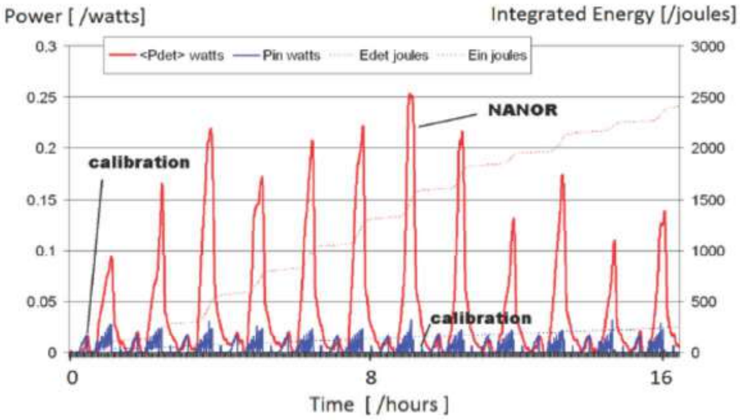

Figure 4. Subsequent late-term impact of magnetization on CF/LANR activity. The post-magnetization electrical input power and energy and output power and heat are shown for the ohmic control and the NANOR®-type component. This experimental run of a M-NANOR®-type component was made several hours after a single application sequence of the fractionated magnetic field was delivered. There was no additional H-field applied for this figure. The peak applied voltage was ~125 V. Note the absence of an exponential or linear fall-off of peak activity.

in incremental power gain and excess energy gain, over ordinary CF/LANR. This magnetization sequence created an increase of ca. 4–10 times the peak power gain over conventional LANR with the same system. The peak power gain of such treated NANOR®s ranged from 22 to up to ~80 times input electrical power or more beyond the control, as determined by calorimetry [4,10,11].

There are also subsequent effects (occurring later, or metachronous) and strong evidence for the first ever-observed two (2) optimal operating point (OOP) manifolds [4]. Some of these dramatic changes can be seen in Fig. 3, which shows the first evidence of magnetic rejuvenation of nanostructured CF/LANR material, and even increasing the CF/LANR activity to higher levels than observed initially!

Figure 3 shows a calorimetric presentation of the ohmic control and the NANOR®-type component. It demonstrates the impact of the magnetic field, with no change from the same magnetic field on the background or control. In Fig. 3, the magnetic field intensity was applied only at one point in time which is indicated by the black arrows. At all other points in time, there was NO additional applied magnetic field intensity. Note the synchronous amplification of the M-NANOR® power output induced by the magnetic field. This is not seen in the ohmic control.

3.2.3. *Metachronous magnetically induced increased energy gain*

Other effects were noted. Astonishingly, after the single application of the fractionated large applied magnetic field intensity was delivered at one point in time (between the arrows), there is improvement in the CF/LANR activity which also appears later – long after the initiation of the magnetization [4]. This metachronous impact wrought upon the treated CF/LANR M-NANOR®s, long after the treatment, is heralded as increased power and energy gain as determined by delta-T/P_{in}, delta-HF/P_{in}, and calorimetry. Subsequent, metachronous effects are those physical changes wrought by the applied high intensity fractionated magnetic field *after* the field was applied.

Figure 4 is a calorimetric presentation of a different run later many hours after the single application of the fractionated large applied magnetic field intensity was delivered. In Fig. 4, many cycles are shown which demonstrated clearly that there was more output than the ohmic control, and as astonishingly, there is improved activity which is shown here to be metachronous and long-lasting. Notice that the peak power gain of the M-NANOR®-type component is increased *after* the application of the fractionated large applied magnetic field intensity.

3.2.4. *Magnetically induced activity has an oscillation of activity*

There are other remnant effects long after the application of the H-field. These late-appearing effects include an increased, but variable, activity. The subsequent activity of the magnetized M-NANOR®-type components no longer decreases in a simple regular, evanescent manner over time (as described in previous publications [1–5]); but instead appears irregular with a periodic component, as first seen in Fig. 3 and also shown in Fig. 4. The cyclic component of the activity in in the range of circa 1.3×10^{-4} Hz ($0.2–5 \times 10^{-4}$ Hz).

3.2.5. *Magnetically induced unique dual optimal operating manifolds (OOPs)*

Although not covered in detail here, previously, all CF systems and the NANOR®s had shown a single optimal operating point manifold for excess heat operation, ^{4}He production, and other products [15,14,4]. Today, that is no longer accurate. Even after a single treatment to a high intensity fractionated magnetic field, there arise two OOP manifolds. The new OOP is elicited at higher input electrical power, and so the new, second, OOP is located to the "right" of the conventional, first, CF/LANR OOP [4]. Although this revelation is far beyond the scope of this paper, its impact is very important because magnetically activating preloaded nanostructured CF/LANR devices is both very useful [4] and instructive [8]. Although cold fusion (LANR) has a first stage mediated by phonons within the loaded lattice by coherent Phusons [18], there is also a magnetically coerced second stage, which we believe may be mediated by magnons, or interactions of phonons in H-field and included magnetization field.

4. Interpretation

4.1. Possible implications of magnetized domains

The unique temporal changes, shown in Figs. 3 and 4, and the amplification of CF/LANR excess heat by fractioned magnetic fields effects suggest a new CF/LANR material science/nuclear interaction. The analysis below is thus important because the magnetic domains, magnetic interactions, magnetically increased incremental power gain, might be relevant to other materials and other systems.

4.2. Magnetism in ZrO_2–Pd/Ni and ZrO_2–Pd components

How can palladium become magnetic? Nickel is ferromagnetic and the induction of magnetization is to be expected. So this is expected for the nickel-containing NANOR®s, but it is somewhat surprising for the palladium M-NANOR®s. However, palladium like platinum, has potential capacity as an exchange-enhanced paramagnetic materials to exhibit a strong Stoner enhancement and become ferromagnetic upon tension [19]. When the Stoner criterion is satisfied, in response to external stimuli such as applied E-field, the materials can exhibit unconventional magnetic responses – they become exchanged-enhanced ferromagnetic.

Thus, the solid state metallurgical lattice of Pd can become ferromagnetic or its equivalent post-magnetization. This has now been seen [20] and confirmed in magnetic domain scanning and imaging which will be the subject of an upcoming paper (cf. also Fig. 5).

The magnetization and oscillations may also be consistent with other reports of quantum oscillations in several systems, including metallic triangular-lattice antiferromagnet $PdCrO_2$ [21], and as seen in the (electrically tunable) anomalous Hall effect observed in platinum thin films [22], as seen with both lattice and magnetic oscillations in stacks of Josephson junctions [23], and with reports of excess energy production with high voltage magnetic pulses coerced through nanograined magnetic materials such as strontium ferrites [24]. The coerced magnetization is important and may also be consistent with some of those materials considered theoretically in investigations using DFT calculations of strained ferromagnetic lattices [25].

4.3. Interaction forces between magnetized domains

It is important to consider the material science and metallurgy of this new magnetic behavior and material(s) (Fig. 5). From what do the domains arise, and how do they interact. How can the magnetic domains couple and account for the unusual time-variant activity? Magnetic materials can self-interact, as described by the Langevin function [26]. Theoretically, this is supported by density-functional calculations [27]. Most interestingly, this appears to be driven by vacancies in Pd (theoretically, up to 15% calculated using the SCR Korringa–Kohn–Rostoker coherent potential approximation method, which predicts a magnetic moment at ~10% vacancies) [28]. Attention is drawn to the interesting fact that several theories of cold fusion also require vacancies [29].

5. New Hypothesis. Is Oscillation of Activity Linked to Magnetized Domains

The continuum electromechanical equations may give a possible new understanding of the just-discovered time-varying activity change that appears in post-magnetized components [4]. This is important because these changes are uniquely different from observations of hundreds of runs on scores of samples. These M-NANOR®-type components have responded markedly differently, requiring this attempt to mathematically analyze, and possibly explain, this

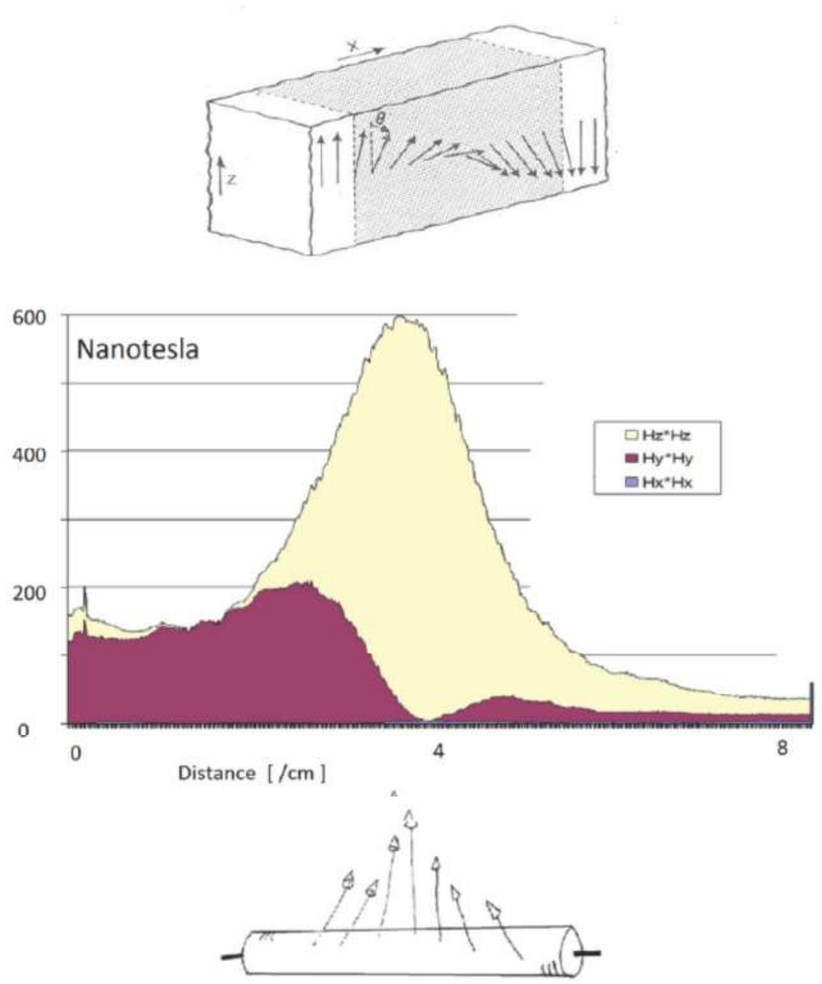

Figure 5. Magnetic Domains in NANOR®-type components. (*top*) Schematic showing magnetic domains interacting within a lattice. The magnetization is observed changing over a distance (after John Mara and A.von Hippel [32]. (*bottom*) These magnetic domains have been observed experimentally and their imaging, and possible implications, are the focus of a manuscript [20]. The graph shows the vectorial scanned magnetization from the domain (in nanotesla) as a function of distance along the long axis of the M-NANOR® 7-8 at rest, long after it was previously operated. The square of each of the x-, y-, and z-axis components are shown as a function of x-axis. (*bottom inset*) Estimated vectorial magnetization along, and just vicinal to, the body of M-NANOR® 7-8.

new post-magnetization observation. The activity oscillations observed in the output excess power of M-NANOR®-type components long after their magnetic field interaction must result from the applied magnetic field intensity. So what is the impact of the H-field on any magnetic domains there? We have begun to measure them in M-NANOR®s after magnetization [20] as shown in Fig. 5.

In this report, we examine the behavior of the oscillating excess heat activity of magnetized M-NANOR®-type components, and attempt to link that behavior to loco-regional magnetic domains in the treated coerced lattice to understand the very unique observed responses of these magnetically treated components. Although better models for, and a solution to, this observation are needed, this is a first approximation.

These domains can be modeled as a remnant magnetization of the lattice, and here are taken into account through the forces and tension they incur through the density of the lattice and Poisson's ratio. Specifically, using the findings of strained layer ferromagnetism in transition metal, it is found that tension increases magnetization and simultaneous should decrease density [25], and these may be the conditions that give rise to the activity oscillations.

6. New Results. Magnetic Forces and Oscillations from CF/LANR Domains

To model the interactions of two neighboring magnetic domains, we assume that in addition to the normal mechanical restoring forces that there are also electromechanical forces. We begin the analysis with Newton's equation, using a continuum model using a simple spring constant equation for the initial analysis.

$$\frac{\mathrm{d}^2 x}{\mathrm{d}t^2} = \frac{F}{M}. \tag{1}$$

The magnitude of the restoring force is derived using Hooke's law augmented by the Maxwell stress tensor which is integrated over the surface boundary between those two magnetic domains to derive the volume-integrated induced force [30–32].

The force density, in integral and differential forms, thus becomes

$$\int_V \left[-\frac{1}{2}\mathbf{H}\cdot\mathbf{H}\nabla\mu + \nabla\left(\frac{1}{2}\mathbf{H}\cdot\mathbf{H}\frac{\partial\mu}{\partial\rho}\rho\right) - \mathbf{F}\right]\cdot\delta\xi\,\mathrm{d}V = 0, \tag{2}$$

$$\mathbf{F} = -\frac{1}{2}\mathbf{H}\cdot\mathbf{H}\nabla\mu + \nabla\left(\frac{1}{2}\mathbf{H}\cdot\mathbf{H}\frac{\partial\mu}{\partial\rho}\rho\right). \tag{3}$$

Therefore, the force, and the stress tensor, would there be, and derived as follows:

$$F_{\mathrm{m}} = \frac{\partial T_{mn}}{\partial x_n}, \tag{4}$$

$$T_{mn} = \mu H_n H_m - \frac{1}{2}\delta_{mn}H_k H_k\left(\mu - \frac{\partial\mu}{\partial\rho}\rho\right). \tag{5}$$

Note the magnetoelectric term at the end (reminiscent of electrical dielectrophoresis). Substitution in the original equation, with terms including magnetostriction, gives

$$M\frac{\mathrm{d}^2 x}{\mathrm{d}t^2} = -\left[\mathbf{K}\ \times\ \mathrm{x}\right] - \frac{[Bo]^2}{2\times\mu^2}\left[\Delta\mu + \left[(-\Delta\rho)\left(\frac{\delta\mu}{\delta\rho}\right)\right]\right]. \tag{6}$$

The solution has an amplitude of

$$\frac{[Bo]^2}{2V\rho\mu^2 K\sqrt{(\omega_0^2-\omega^2)}}\left[\Delta\mu + \left[(-\Delta\rho)\left(\frac{\delta\mu}{\delta\rho}\right)\right]\right] \tag{7}$$

and a natural frequency of

$$\omega_0 = \sqrt{\frac{K}{\rho V}}. \tag{8}$$

This might be the resultant natural frequency which we see in the M-Nanor®'s excess energy cyclic activity (cf. Figs. 3 and 4).

7. Conclusion. Oscillating Activity and Magnetic Domains

There are two types of NANOR®-type CF/LANR components. They have very different behavior. The post-magnetization effects are significant and time-variant because it has now been discovered that high intensity, dynamic, repeatedly fractionated, magnetic fields have an incremental major, significant and unique, complex, metachronous amplification effect on preloaded M-NANOR®-type LANR devices.

Furthermore, in contrast to previously observed exponential falloffs of sample activity (peak incremental excess power gain), post-magnetization activity demonstrates oscillatory activity, and the Maxwell stress tensor heralds a theoretical frequency for oscillations now observed to exist between these magnetic domains in these magnetized NANOR®-type components. The observed frequencies of activity change observed appear be circa 1.3×10^{-4} Hz (range $0.2–5 \times 10^{-4}$ Hz).

This paper's analysis of the force density, calculated by using the Maxwell stress tensor, predicts oscillations now observed to exist between these magnetic domains in these magnetized NANOR®-type components. This analysis indicates that magnetic interactions between domains should augment other restoring forces, and that the frequency should increase with decreasing mass, and increasing applied magnetic field intensity (presumably until coercion effects elicit no further increase). It is important to consider this new material science and metallurgy with surprising new magnetic behavior in future analyses and experiments.

Acknowledgments

The author acknowledges and thanks Gayle Verner and Alex Frank for their very helpful editorial support. The author is grateful to and thanks the teams who have helped collect the data, support the work, and have helped better understand the physics and materials with their assistance, ideas and suggestions including Richard Goldbaum, Jeffrey Tolleson, Gayle Verner, Leslie Wright, Linda Hammond, Alex Frank, Alan Weinberg, Charles Entenmann, Allen Swartz, Joshua Gyllinsky, Peter Hagelstein, Florian Metzler, Brian Ahern, Jeff Driscoll, Dennis Cravens, Pamela Mosier Boss, Lawrence P.G. Forsley, Frank Gordon, Louis DeChiaro, and Dennis Letts. This effort was supported by JET Energy Inc. and the New Energy Foundation. NANOR® and PHUSOR® are registered trademarks of JET Energy, Incorporated. NANOR®-technology, and PHUSOR®-technology are protected by U.S. Patents D596724, D413659 and several other patents pending.

References

[1] M.R. Swartz, G. Verner, J. Tolleson and P. Hagelstein, Dry, preloaded NANOR®-type CF/LANR components, *Current Sci.* **108** (4) (2015) 595.

[2] M.R. Swartz and P.L. Hagelstein, Demonstration of energy gain from a preloaded ZrO_2–PdD nanostructured CF/LANR quantum electronic device at MIT, *J. Condensed Matter Nucl. Sci.* **13** (2014) 516. www.iscmns.org/CMNS/JCMNS-Vol13.pdf.

[3] M.R. Swartz and P.L. Hagelstein, Demonstration of energy gain from a preloaded ZrO_2–PdD nanostructured CF/LANR quantum electronic device at MIT, *J. Condensed Matter Nucl. Sci.* **13** (2014) 516. www.iscmns.org/CMNS/JCMNS-Vol13.pdf.

[4] M.R. Swartz, G.M. Verner, J. Tolleson, L. Wright, R. Goldbaum and P.L. Hagelstein, Amplification and restoration of energy gain using fractionated magnetic fields on ZrO_2–PdD nanostructured components, *J. Condensed Matter Nucl. Sci.* **15** (2015) 66. www.iscmns.org/CMNS/JCMNS-Vol15.pdf.

[5] M.R. Swartz, Incremental high energy emission from a ZrO_2–PdD nanostructured quantum electronic component CF/LANR, *J. Condensed Matter Nucl. Sci.* **15** (2015) 92. www.iscmns.org/CMNS/JCMNS-Vol15.pdf.

[6] M.R. Swartz, G. Verner, J. Tolleson, L. Wright and R. Goldbaum,, Imaging of an active NANOR®-type LANR component using CR-39, *J. Condensed Matter Nucl. Sci.* **15** (2015) 81. www.iscmns.org/CMNS/JCMNS-Vol15.pdf.

[7] M.R. Swartz, P.L. Hagelstein and G. Verner, Impact of electrical avalanche through a ZrO_2–NiD nanostructured component on its incremental excess power gain, ICCF-19, *J. Condensed Matter Nucl. Sci.* **19** (2016) 287–297.

[8] M.R. Swartz, Detection of phonon gain from a NANOR®-type CF component (2016, in preparation and review).

[9] M.R. Swartz and G. Verner, Excess heat from low electrical conductivity heavy water spiral-wound Pd/D_2O/Pt and Pd/D_2O-$PdCl_2$/Pt devices, *Condensed Matter Nuclear Science, Proc.ICCF-10*, World Scientific, Singapore, ISBN 981-256-564-6, 29-44; 45–54 (2006).

[10] M.R. Swartz, Excess power gain using high impedance and codepositional LANR devices monitored by calorimetry, heat flow, and paired stirling engines, *Proc. ICCF14* **1** (2008) 123; ISBN: 978-0-578-06694-3, 123 (2010). www.iscmns.org/iccf14/ProcICCF14a.pdf.

[11] M.R. Swartz, Survey of the observed excess energy and emissions in lattice assisted nuclear reactions, *J. Scientific Exploration* **23**(4) (2009) 419–436.

[12] J. Marwan, M.C.H. McKubre, F.L. Tanzella, P.L. Hagelstein, M.H. Miles, M.R. Swartz, E. Storms, Y. Iwamura, P.A. Mosier-Boss and L.P.G. Forsley, A new look at low-energy nuclear reaction (LENR) research: a response to Shanahan, *J. Environ. Monit.* **12**(9) (2010) 1765–1770.

[13] M.R. Swartz, G. Verner, A. Frank and H. Fox, Importance of non-dimensional numbers and optimal operating points in cold fusion, *J. New Energy* **4** (2) (1999) 215–217.

[14] D. Cravens, Factors affecting success rate of heat generation in CF cells, *Proc. ICCF-4*, Maui, Hawaii, July 1994, pp. 18-1 through 18-14.

[15] S. Szpak, P.A. Mosier-Boss and F.E. Gordon, Further evidence of nuclear reactions in the Pd/D lattice: emission of charged particles, *Naturwissenschaften* **94** (2007) 511–514.

[16] M.R. Swartz, Impact of an applied magnetic field on the electrical impedance of a LANR device, *JCMNS*, Volume 4, *Proc.,* March 2010, New Energy Technology Symposium held at the 239th American Chemical Society, San Francisco, 2011.

[17] J. O'M. Bockris, R. Sundaresan, D. Letts and Z.S. Minevski, Triggering and structural changes in cold fusion electrodes, *Proc. ICCF4*, Maui, Hawaii, July 1994, 1–46.

[18] M.R. Swartz, **P**husons in nuclear reactions in solids, *Fusion Technol.* **31** (1997) 228–236.

[19] D.L.R. Santos, P. Venezuela, R.B. Muniz and A.T. Costa, Spin pumping and interlayer exchange coupling through palladium, *Phys. Rev.* B **88** (2013) 054423.

[20] M.R. Swartz, Scanning vector magnetometry of NANOR®-type components, in preparation.

[21] J.M. Ok, Y.J. Jo, K. Kim, T. Shishidou, E.S. Choi, H.J. Noh, T. Oguchi, B.I. Min and J.S. Kim, Quantum oscillations of the metallic triangular-lattice antiferromagnet $PdCrO_2$. 3. *Phys Rev Lett.* (2013);111(17):176405 (2013).

[22] Shimizu Sunao, Kei S. Takahashi, Takafumi Hatano, Masashi Kawasaki, Yoshinori Tokura, and Yoshihiro Iwasa, Electrically tunable anomalous hall effect in Pt thin films*, Phys. Rev. Lett.* **111** (2013) 216803.

[23] Lattice configurations and magnetic oscillations in stacks of Josephson junctions, http://mti.msd.anl.gov/homepages/koshelev/projects/mag-osc.htm.

[24] Brian Ahern on the late Arthur Manelas; personal communication (2015).

[25] Louis DeChiaro, L. Forsley and P.A. Mosier-Boss, Strained layer ferromagnetism in transition metals and its impact upon low energy nuclear reactions, *J. Condensed Matter Nucl. Sci.* **17** (2015) 1–26.

[26] Shimizu, Sunao, Kei S. Takahashi, Takafumi Hatano, Masashi Kawasaki, Yoshinori Tokura and Yoshihiro Iwasa, Electrically tunable anomalous Hall effect in Pt thin films, *Phys. Rev. Lett.* **111** (2013) 216803.

[27] Y. Sun, J.D. Burton and E.Y. Tsymbal, Electrically driven magnetism on a Pd thin film, *Phys. Rev.* B **81** (2010) 064413.

[28] N. Takanol, T. Kai, K. Shiiki and F. Terasakil, Effect of copious vacancies on magnetism of Pd, *Solid State Commun.* **97**(2) (1996) 153–156.

[29] M.R. Swartz and P.L. Hagelstein, Transient vacancy phase states in palladium after high dose-rate electron beam irradiation, *J. Condensed Matter Nucl. Sci.* **14** (2014) 50.

[30] J.R. Melcher, *Continuum Electromechanics*, MIT Press, Cambridge, 1981. ISBN-10: 026213165X; ISBN-13: 978-0262131650.

[31] H.H. Woodson and J.R. Melcher, *Electromechanical Dyanamics*, Wiley, New York, 1968.

[32] A.R. von Hippel, *Molecular Science and Molecular Engineering*, MIT Press, Cambridge, 1959.